Design and testing of the GNC for the HERACLES Lunar Ascent Element

T. V. Peters[(1)], J. F. Briz Valero[(1)], P. Arroz Serra[(2)], P. Lourenço[(2)], F. Cometto[(3)], M. Berga[(3)], J.-A. Perez Gonzalez[(4)], A. Cuffolo[(4)], A. Cropp[(5)]

[(1)] GMV, calle Isaac Newton 11, 28760 Tres Cantos, Spain, +34 918077645, tpeters@gmv.com
(2) GMV, Alameda dos Oceanos, n.º 115, 1990-392 Lisboa, Portugal, +351 213829366, parroz@gmv.com
[(3)] Thales Alenia Space Italia, Str. Antica di Collegno, 253, 10146 Torino TO, Italy, +39 0117180370, ferdinando.cometto@thalesaleniaspace.com
[(4)] Thales Alenia Space France, 5 Allée des Gabians, 06150 Cannes, France, +33 492926830, jose-alvaro.perez-gonzalez@thalesaleniaspace.com
[(5)] ESA/ESTEC, Keplerlaan 1, 2200 AG Noordwijk, The Netherlands, +31 715658797, alexander.cropp@esa.int

ABSTRACT

This paper describes the design and testing of the rendezvous GNC for the HERACLES Lunar Ascent Element (LAE). The LAE needs to carry samples from the lunar surface to the Lunar Orbital Platform – Gateway (LOP-G) from where the samples are eventually transported back to Earth. The GNC design integrates the GNC for the launch and ascent, the orbit transfer manoeuvres and rendezvous in a near-rectilinear halo orbit (NRHO) into a single simulator. The main focus of this paper is on the consolidated Monte Carlo simulation test campaign results, in particular the rendezvous phase. A discussion of the results and an analysis of the dependence of the results on the assumptions made to define the scenario is performed. The results show that the current design for the GNC is feasible and that the HERACLES LAE mission to the LOP-G can be successfully performed.

1 INTRODUCTION

Figure 1 shows the HERACLES Sample Return Mission scenario featuring the LAE. The HERACLES landing site is close to the South Pole, in the Schrödinger region #1 (141.33º E 75.47º S). Schrödinger region #2 (141.89º E 75.30º S) is a back-up landing site. The Robotic Landing Stack consists of the Lunar Descent Element (LDE), the Lunar Ascent Element (LAE), a Rover, the Rover Garage Element (RGE) and a sample container. The rover is deployed and starts its mission to explore and collect samples with support from ground and from crew on-board the LOP-G station. The rover places the samples in a sample container that is loaded onto the LAE. The LAE is launched from the lunar surface and carries the samples to the LOP-G station. At the LOP-G station the samples are transferred to the Orion capsule which transports the samples back to Earth.
The LAE thruster configuration consists of 1 main engine, four auxiliary thrusters and eight RCS thrusters. The main engine provides 6 kN in the +z direction and the four 220 N auxiliary thrusters provide thrust approximately in the +z direction. Eight 10 N RCS thrusters provide roll control during the ascent and main engine burn phases, and 6 DOF force torque capability during cruise and rendezvous. The LAE uses star trackers and an IMU for nominal inertial navigation, with Sun sensors for contingency inertial navigation. For the relative navigation the LAE uses a Narrow

Angle Camera (NAC) with a field of view of 5° and a Wide Angle Camera (WAC) with a field of view of 18° for relative navigation at close range.

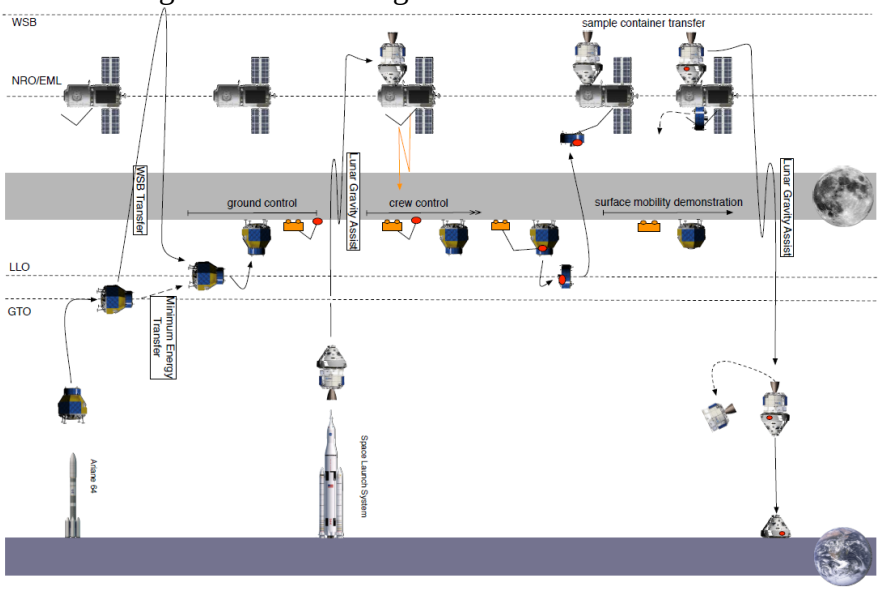

Figure 1: HERACLES Sample Return Mission scenario featuring the LAE

During the first phase of the project, tools were created for analysing near-rectilinear halo orbits (NRHO's) in the Earth-Moon system [1]. These tools are based on multiple-shooting algorithms that use a halo orbit as a seed, and that expand the halo orbit family by means of a continuation method [2], [3]. These tools were used to perform the mission analysis summarized in section 2. The second phase of the project focused on designing and developing the guidance, navigation and control software for the launch and ascent, orbit phasing and for the rendezvous phases. The GNC design is presented in section 3. Section 4 describes the results of the test campaign of the GNC software, with a focus on the orbit transfer and the rendezvous phases of the mission. The test campaign concluded with a HIL test of the final phase of the rendezvous in the ***platform-art***© test facility at GMV. Section 5 describes the results of this test campaign and compares the results to the software-based test campaign described in section 4. Section 6 provides a further discussion and analysis of the overall study results, and section 7 provides the general conclusions that were derived from the GNC design activity.

2 MISSION OVERVIEW

The baseline LAE mission can be summarized in the following phases:

- Pre-Launch. The LAE is prepared for flight on the launch site, checking the correct functioning of the whole system before lift-off
- Launch and Ascent. Starts with launcher lift-off and finishes when the LAE reaches the transfer orbit. The ascent is performed indirectly in 3 consecutive steps or mission arcs:
- Ascent from the Moon landing site into an Elliptical Low Moon Orbit (ELMO)
- Circularisation into a Circular Low Moon Orbit (CLMO)
- Ascent from the Circular Low Moon Orbit into the NRO orbit
- Orbit Transfer and Phasing. The LAE performs the transfer from the launch orbit to the orbit of the LOP-G, carrying out a phasing with the target spacecraft.
- Rendezvous and Forced Translation. The LAE performs a rendezvous with the LOP-G, evaluates its relative attitude dynamics state and performs a forced translation in order to reduce the relative motion to levels adequate to initiate the berthing
- Berthing. The LAE performs a final approach to the target to the distance required to initiate operation of the berthing robotic arm mounted at the LOP-G. This phase is complete when

the LAE has been transferred to its final mating location and the robotic arm has been uncoupled from the LAE.

Table 1 shows a high-level timeline for the Heracles LAE mission summarizing the steps outlined above.

Table 1: HERACLES LAE MISSION TIMELINE

Phase	Sub-phase	Activity	Initial conditions	Final conditions	Time	Remarks
LEOP	Pre-launch	-	start of pre-launch sequence	GO for launch		
	Launch		GO for launch	ELMO insertion	~5 min	
	free drift to apogee		ELMO insertion	ELMO close to apogee @ 100 km	40 min	
	Orbit circularization		ELMO close to apogee @ 100 km	100 km circular LLO	seconds to minutes	few 10's of m/s of delta-V, performed using coarse RCS
Orbit Transfer and Phasing	Phasing in LLO	Ground tracking & orbit determination	100 km circular LLO	Optimal conditions for TIM	few days	
	Orbit transfer injection manoeuvre	De-spin, repoint, perform manoeuvre, repoint and spin-up	Optimal conditions for TIM	TIM complete	~1 min	
	Free drift	Ground tracking & orbit determination	TIM complete	Scheduled time for TCM reached	24 h	
	Orbit transfer correction manoeuvre	De-spin, repoint, perform manoeuvre, repoint and spin-up	Scheduled time for TCM reached	TCM complete	~1 min	
	Free drift	Ground tracking & orbit determination	TCM complete	Scheduled time for NIM reached	~36h	target detection may occur at >1000 km

Phase	Sub-phase	Activity	Initial conditions	Final conditions	Time	Remarks
	NRO insertion manoeuvre	execute insertion manoeuvre	Scheduled time for NIM reached	NIM complete; NRO 50 km below, 141 km behind	~1 min	terminal distance 150 km away from the target, drifting towards the target
Rendezvous	Far rendezvous	Drift in low NRO, search for target, impulsive manoeuvres to S2.1	NRO 50 km below, 141 km behind	S2.1 @ 4.5 km	~10h	NAC ranging possible from S2.1
	Mid-range rendezvous	impulsive manoeuvres to S3	S2.1 @ 4.5 km	S3 @ 200 m	~2h	NAC model based tracking
	Close rendezvous	Forced motion to S3	S3 @ 200 m	S4.1 @ 35 m	~30 min	Fiducial marker tracking; start of relative attitude availability; start of forced motion guidance modes
	Terminal rendezvous	Forced motion to S4.3 (terminal hold point	S4.1 @ 35 m	S4.3	~30 min	transition from LVLH to body frame occurs at S4.1
	Berthing	Extend robotic arm, grapple LAE, move LAE to terminal position, mate LAE, disconnect robotic arm	S4.3, telecommand received	LAE mated, robotic arm disconnected	Up to 50 min	LAE mated

2.1 Launch and ascent

A nominal ascent trajectory starting from the Schrodinger Crater (-75° N, 132.4° E) has been generated. The trajectory design parameters are as follows:

- Target periselene – 30 km
- Target aposelene – 100 km
- Inclination – 80 °
- Engine Thrust – 6 kN
- Specific Impulse – 340 s
- Dry Mass – 451.83 kg
- Propellant Mass – 659 kg

Figure 2 shows the altitude of the ascent trajectory.

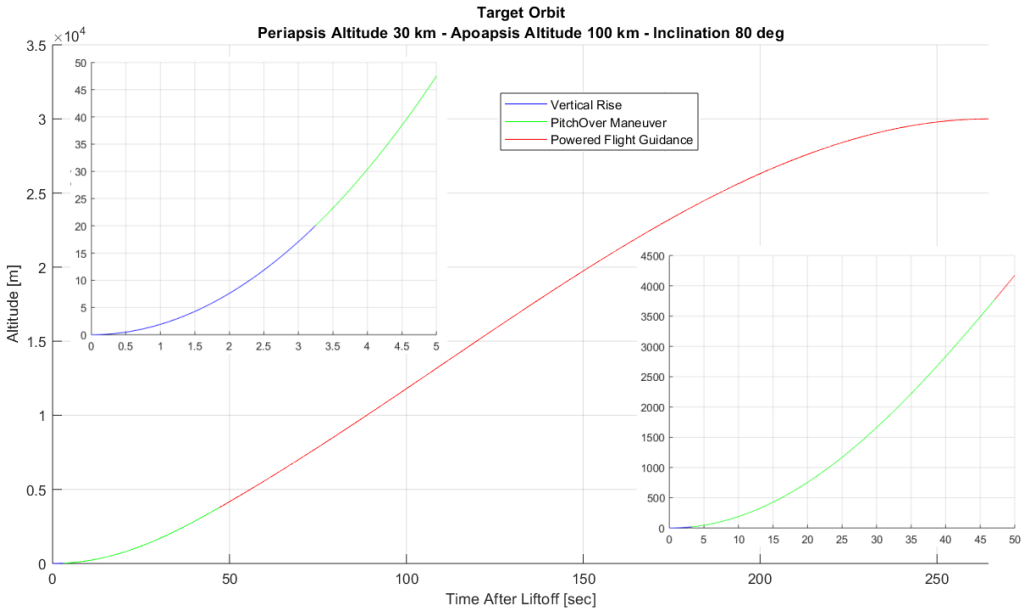

Figure 2: Ascent trajectory. Altitude (30x100)

2.2 Phasing

The orbit transfer phase consists on a single transfer injection manoeuvre (TIM) with a single trajectory correction manoeuvre (TCM) to reduce the effect of errors in navigation and manoeuvre execution at the moment of the TIM. The calculation of the transfer manoeuvre is performed as follows:

1. The initial state and the terminal state are transformed to the Moon-centred inertial frame. The initial state is determined by means of orbit determination from ground. The terminal state is determined by the ephemeris of the station plus a fixed offset. The transfer time and the fixed offset are parameters to the algorithm. The value of the transfer time parameter is set to the value determined by mission analysis.
2. A two-body Lambert solver is used to find an initial guess for the initial velocity in the Moon-centred inertial frame.
3. The initial state vector is transformed from the Moon-centred inertial frame to the Earth-Moon barycentric inertial frame
4. A differential correction process is used to correct the ΔV. The differential corrector is essentially a single-shooting algorithm. This means that the variational equations are integrated along with the initial state vector, and the state transition matrix is used to correct the initial velocity.

One mission objective is to maximize surface operations but launching before sunset to ensure

batteries are fully charged for the ascent phase. The analysis has considered a range of 7 days before sunset as available ascent dates. The left image of Figure 3 shows the subsolar point (in red) in the available dates, where Shackleton crater is illuminated. Once the LAE has ascended and has been introduced into an LLO, a loitering period is introduced to match the orbital plane of the LLO with the NRO trajectory. This loitering period allows a reduction in TIM ΔV by making the LLO velocity tangent to the TIM ΔV manoeuvre applied. From a frame rotating with the Earth-Moon system, the NRO is fixed and the LLO rotates with a rate of 13 ° per day, displayed in Figure 3. In the analysis, a minimum loitering interval of 1 day is considered to allow for ground orbit determination, while the maximum loitering interval considered is 5 days to ensure stability of the LLO in the gravity field of the Moon.

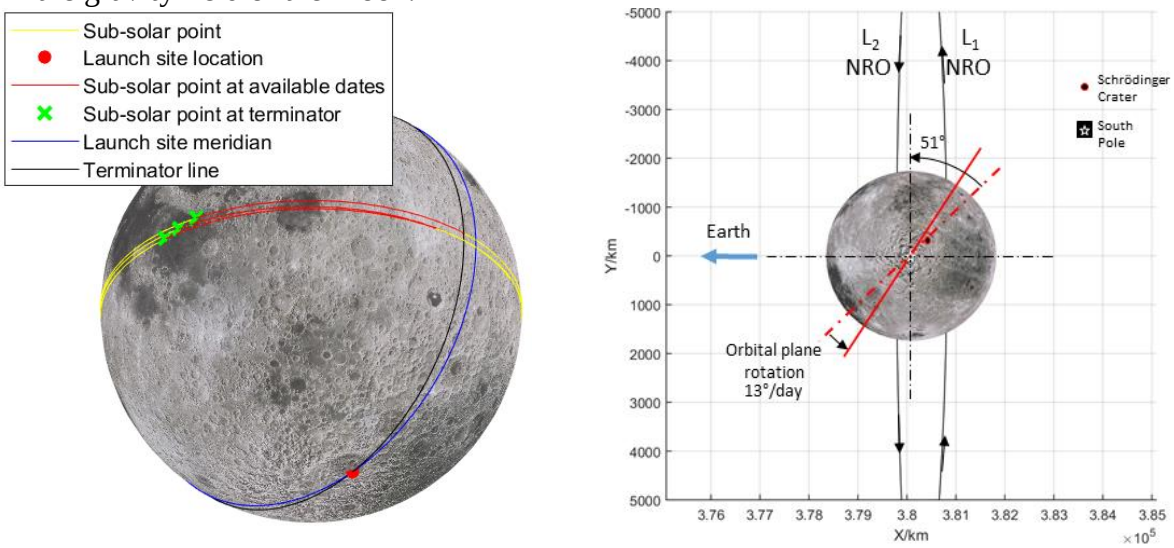

Figure 3: Ascent constraints and loitering

The arrival in the NRO places the LAE at a distance of 150 km from the LOP-G station. Under the assumptions of the ground-based navigation accuracy and the trajectory dispersions at the end of the transfer arc, the LOP-G station will be within the 5° field of view of the narrow angle camera. This means that the LAE can detect LOP-G without performing an attitude-scanning search manoeuvre.

2.3 Rendezvous

The last segment of the transfer from LLO to halo and the rendezvous cover only a small fraction of the orbital period, such that the dynamics is very slow. That is to say, the chaser moves along a trajectory that is nearly a straight line with respect to the target. This means that dynamical coupling of the axes is quite weak. (For LEO rendezvous, by contrast, the motion in the V-bar and R-bar directions of the LVLH frame are dynamically coupled.) The rendezvous with the target is performed as a series of straight-line segments oriented at an angle to each other, Similar to a ship tacking into the wind. This strategy is shown in Figure 4. The objectives of this strategy are:

- To provide passive safety, by ensuring that the chaser does not enter a predefined safety volume if a tack manoeuvre cannot be performed.
- To increase observability of the problem. If the magnitude of the tack manoeuvres can be measured, then the evolution of the line of sight can be combined with the measurements of the ΔV's to determine the full state.
- To reduce plume impingement of the chaser thrusters in the target, by pointing the thruster plumes at an angle with respect to the line of sight from the chaser to the target.

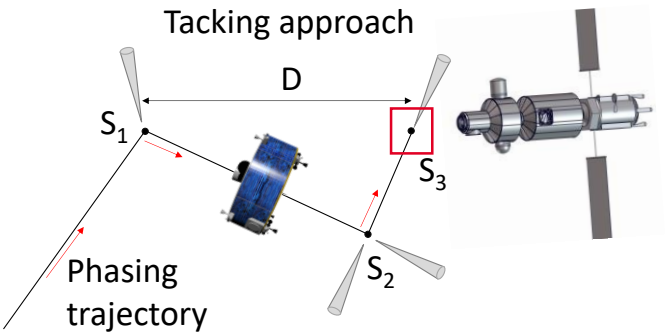

Figure 4: Impulsive rendezvous

Figure 5 shows the final phase of the rendezvous, a forced motion approach. The forced motion approach is defined using a halo-orbit analogue to the familiar local vertical, local horizontal frame. The x-axis, R-bar points down towards the moon, the y-axis, H-bar points in the direction perpendicular to R-bar and the instantaneous halo orbit velocity vector in the synodic frame and the x-axis, V-bar completes the reference frame.

The forced motion approach starts at 200 m to hold point S4.1 at 35 m, performed with respect to the LVLH frame. At point S4.1 the chaser starts tracking the target attitude. The chaser now performs a circular fly-around to point S4.2, roughly on H-bar, and finally a straight-line approach to point S4.3 at 2 m distance from the space station to be captured by means of a robotic arm.

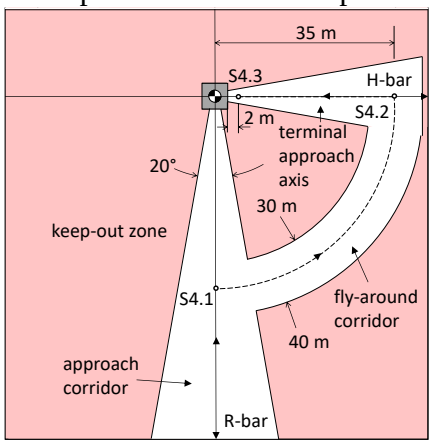

Figure 5: Final forced motion terminal rendezvous

3 GNC DESIGN

Reference [1] provides a general overview of the full design of the GNC system. This article focuses mainly on the rendezvous GNC, for which testing was performed both through Monte Carlo simulations and HIL tests with a camera sensor in the loop. Figure 6 shows the GNC architecture for the HERACLES LAE. The GNC for the launch and ascent, orbit transfer and the rendezvous phases are included as separate modes in the guidance, navigation and control blocks shown in the figure. The MVM block commands mode switching and parameter changes during the entire flight. In addition the MVM commands manoeuvres during all phases of the rendezvous. The MVM commands are based on sequences of plans that have been defined for all phases.

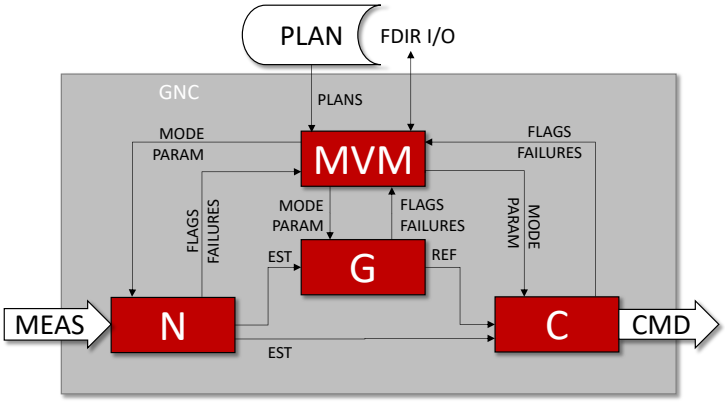

Figure 6: GNC architecture for the HERACLES LAE

Figure 7 shows the proposed approach for the short-range phase image processing and navigation for the NRO-GNC project. Instead of solving the PnP problem [4] directly, the individual marker positions are treated as measurements and tracked by the filter. The relative attitude and position of the LOP-G station are part of the dynamical model in the Kalman filter that predict the expected marker positions in the camera field of view. The marker positions are predicted using the projection equation, represented in the figure as the function f.

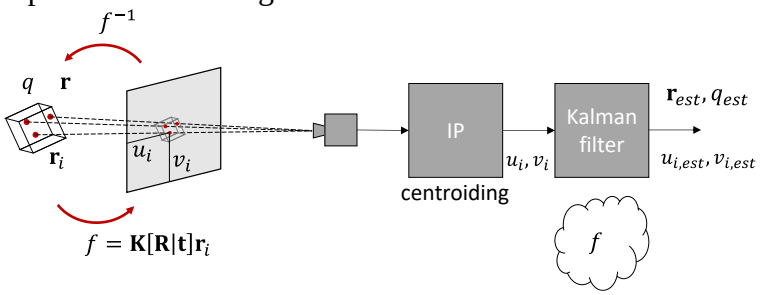

Figure 7: Fiducial marker tracking by means of a filter

The navigation function assumes the dynamics is gravity-free, and that the angular velocity of the target is constant between each observation with the camera. A behavioural model is used for the image processing function for this phase. The behavioural model outputs the locations of the fiducial markers in the camera frame including Gaussian white noise and bias. An in-house investigation has shown that a centroiding algorithm is effective in extracting the positions of the fiducial markers and that the noise is approximately Gaussian. Bias in the position of the markers stems from uncertainties in the knowledge of the placement of the markers.

The translational guidance considers impulsive manoeuvres for long and mid-range phases, and forced motion manoeuvres for short ranges. Considerable effort was spent on ensuring that the guidance trajectory is flexible, meaning that the guidance can respond to commands to advance, stop and retreat during the entire rendezvous. The guidance during the final forced motion is under the direct command of the MVM, which (amongst others) commands the guidance to move between hold points. Figure 8 summarizes the different navigation modes, manoeuvres and hold points in the terminal rendezvous, as well as the connection of hold points through said manoeuvres. In this diagram, “IMP” indicates impulsive manoeuvres, “FMS” indicates straight-line forced motion and “FMA” indicates a forced motion fly-around. The diagram also indicates which navigation mode is active, and what trajectory protection is used during each segment of the trajectory, CAM or safe mode. The guidance was formulated in such a way that the diagram can be followed both in a forward direction and in a backward direction, and the LAE can also be commanded to stop halfway between hold points, before either continuing the advance or retreating.

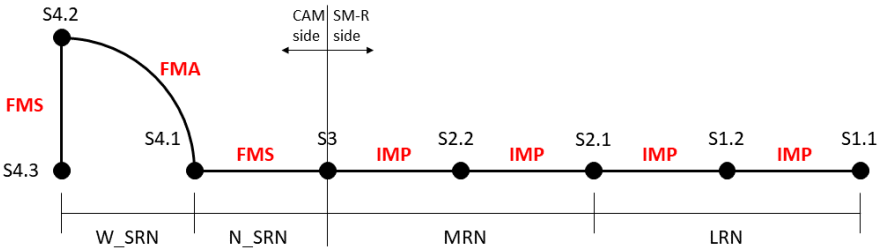

Figure 8: Terminal rendezvous manoeuvres and navigation modes

The closed loop controllers have been synthesized using H_∞ techniques, and assuming that sloshing effects are present (modelled as a mass-spring-damper system), as well as thruster misalignments (including delay, magnitude, and orientation uncertainties).

4 SIMULATION RESULTS

An extensive simulation campaign has been performed to validate the GNC. Simulations were performed that cover all phases described in section 2 (launch, orbit transfer manoeuvres and rendezvous). This paper focuses on the results of the rendezvous phase. The simulation campaign consists of simulations of the nominal case and Monte Carlo simulations that vary crucial parameters of the LAE design, such as for example, the mass parameters, sensor and actuator biases et cetera.

Figure 9 shows the LVLH trajectory. A straight-line approach is performed from 370 seconds to 1070 seconds, followed by station-keeping. At about 1140 seconds, the chaser switches to station-keeping in the target body frame, followed by a fly-around at 1340 seconds. The switch to target body frame starts when the WAC based navigation converges. The fly-around is followed by a brief period of station-keeping between about 1240 seconds and 1740 seconds. The final approach from 35 meters to 5 meters takes place between 1750 seconds and 2050 seconds. At the end of the simulation, the chaser performs about one minute of station-keeping in the target body frame.

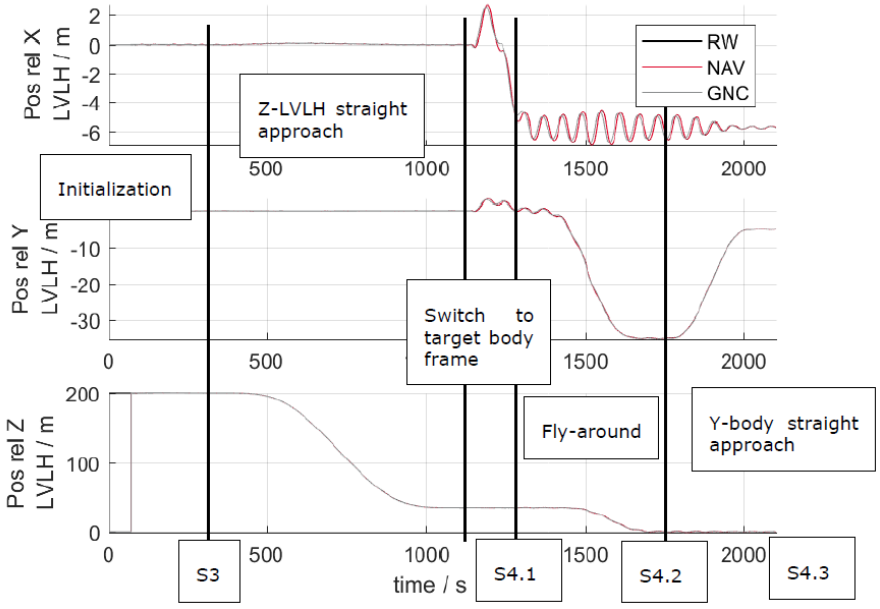

Figure 9: LVLH trajectory during nominal close-range rendezvous

Figure 10 shows the results of the target attitude and position estimation. The estimate is shown in red, and the 3σ bounds are shown in grey. The figure shows that the navigation is only partially successful in estimating the attitude motion of the target; the errors show the same oscillatory behaviour as the target attitude motion. The reason for this is that the navigation assumes the target does not experience any angular acceleration. The behaviour of the filter is expected to improve if

an estimation of the acceleration is included, for example, as a consider parameter in the filter, or if the attitude control of the station would be switched off during the final phase of the rendezvous, leading to much slower evolution of the target attitude.
The relative position and velocity estimation is good. The covariance decreases when the chaser approaches the target (over the z-axis). The switch to the WAC at 1140 seconds can be identified as a jump increase in the 3σ covariance bounds. Next, between 1200 s and 1500 s, the chaser performs a fly-around to the y-axis. This shifts the wider bounds on the position uncertainty from the z-axis to the y-axis. Finally, as the chaser performs the final approach, the covariance on y decreases again. The estimation of the x-coordinate is not as good as the estimation of the y-coordinate. This is caused by the fact that the size of the pattern of markers is larger in the y-direction than in the x-direction. It is expected that if additional markers are added in the x-direction, then the estimation of this coordinate would likely improve. Between 1200 s and 1500 s, the estimates of the position and velocity show an oscillation with an amplitude of 2 cm in position and about 0.5 cm/s in velocity that is directly related to the attitude motion of the target. The errors decrease as the chaser performs the final approach to 5 m.

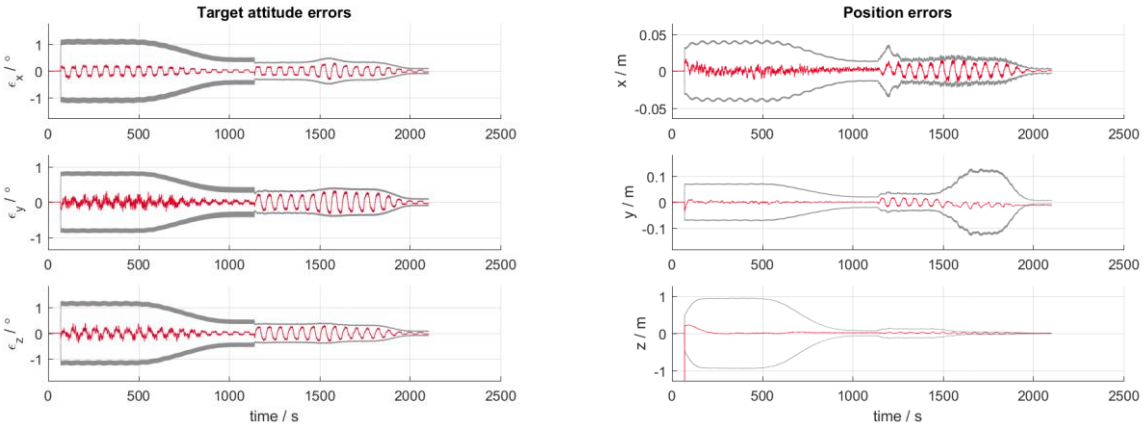

Figure 10: Target attitude and position estimation errors

Figure 11 (left) shows the evolution with time of the full GNC, navigation and control errors. Two main points can be obtained from this image. Firstly, navigation errors are the most important source of errors during the approach in LVLH (up to 1200 s). Secondly, control errors drive the GNC error during the body frame approach (from 1200 s onwards). This motion is complex in nature, and the control error can be explained for two reasons:

- The controller design includes some overshoot to decrease response time. However, this is causing the peaks in body frame motion to be accentuated, increasing the errors.
- The Navigation filter provides the estimated target attitude, angular rate and angular acceleration, which are used by the guidance to compute a feedforward force. However, errors in the estimation of the target motion cause the errors in relative state.

The right-hand side of Figure 11 shows the evolution of the navigation position errors as a function of the distance. The errors decrease with distance.

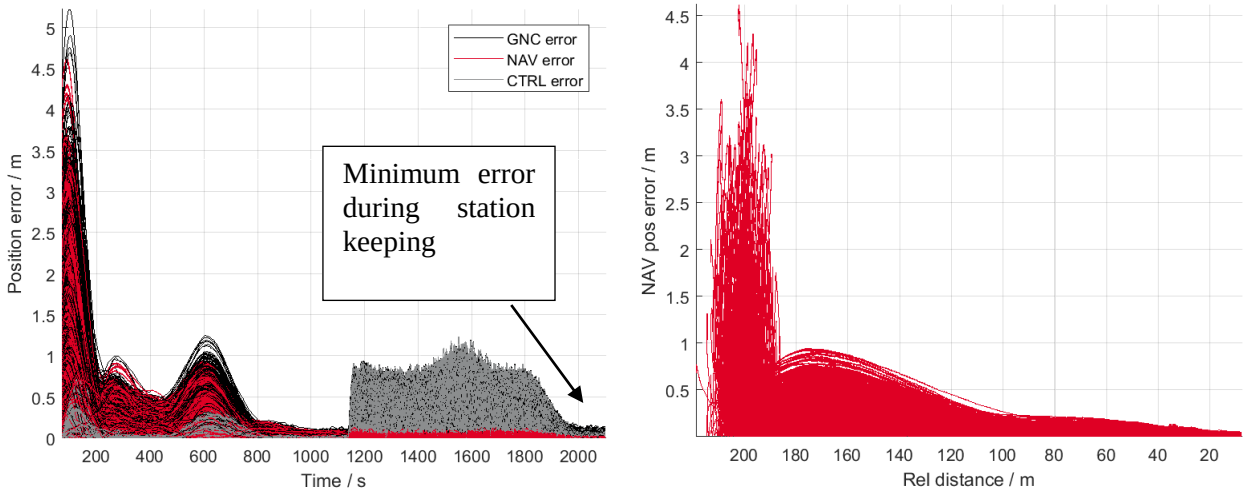

Figure 11: GNC performance in position

Figure 12 shows the GNC errors during the 60 seconds of station-keeping in the berthing box: position (top left), velocity (top right), attitude (bottom left) and angular rate (bottom right). Position, attitude and velocity are respected a 100% of the cases, while the angular rate is not.

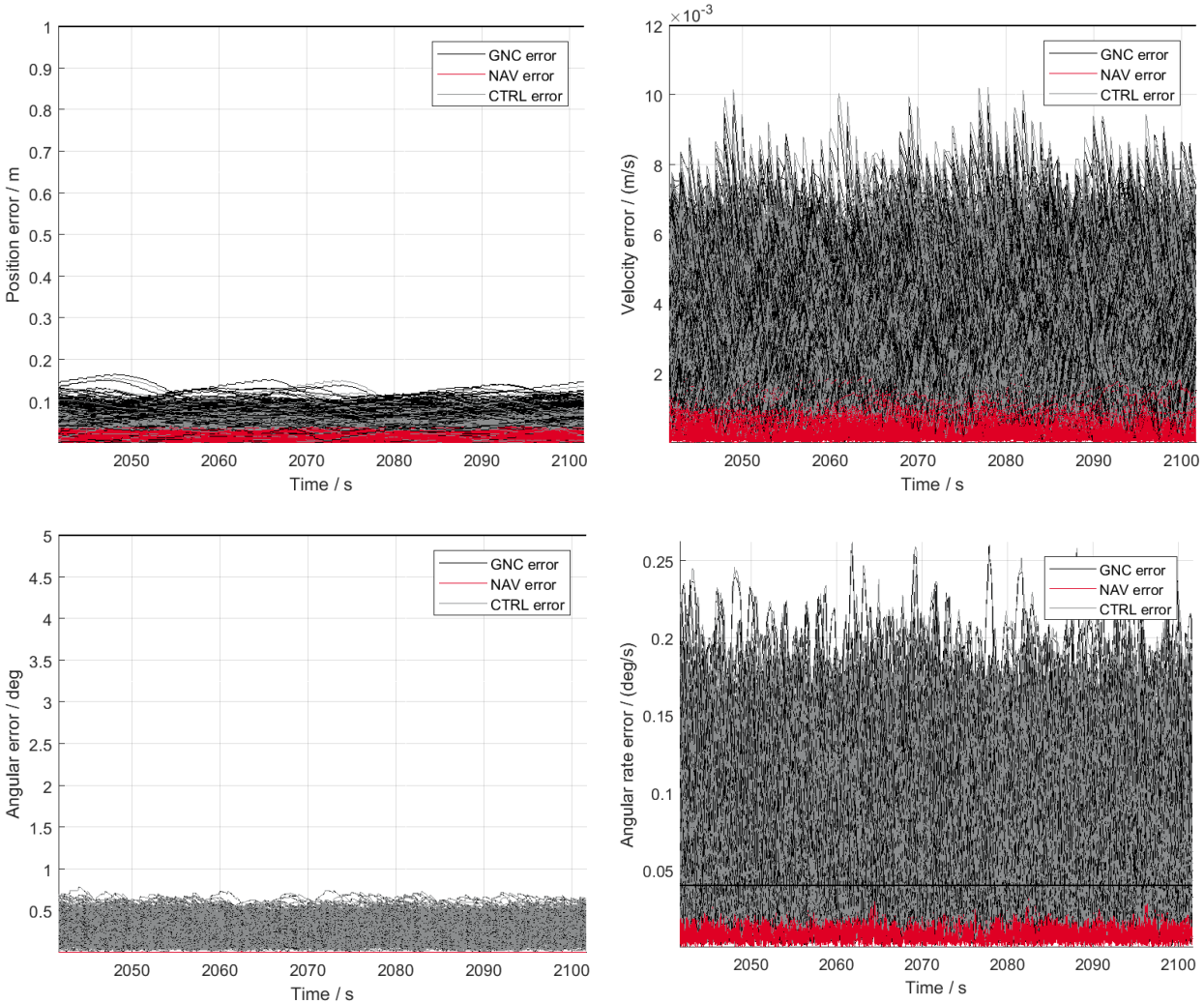

Figure 12: Berthing errors: position, velocity, attitude and angular rate

The high angular velocity error can be explained by the following reasons:

- The navigation errors are fairly high compared to the requirement. This can be explained by the fact that the main observables in attitude are the star tracker (which estimates

attitude) and the observables in attitude are the gyro measurements. The gyro measurements are relatively noisy, and the USQUE filter has a relatively poor steady state error compared to other attitude filters [5]. The attitude rate navigation already accounts for about half of the maximum allowable error.

- The control errors increase the rate error to about 0.2 °/s, compared to a requirement of < 0.04 °/s (3σ). A large component of the acceleration and attitude acceleration required to follow the target attitude comes from the target angular acceleration. This means that the control needs to constantly provide both forces and torques. The minimum impulse bit of the thrusters by itself induces a change in angular velocity that is greater than the requirement.

The requirement on the angular rate is mainly driven by the need to capture the LAE with a robotic arm during berthing. A mission with a similar objective (capture by means of a robotic arm) was studied in the debris removal project ORCO [6]. The ORCO project required a GNC performance of 0.2°/s (or 5 times higher than the limit considered here) in angular rate during attitude synchronization with a tumbling debris object in order to successfully capture the object by means of a robotic arm. Note that a free-tumbling debris object experiences a smaller angular acceleration than what was assumed here, which allows a better performance in attitude rate estimation. Not meeting the requirement on attitude rate during berthing is not considered to be a show stopper at this time. In the context of the HERACLES GNC design work the requirement has been updated to 0.25 °/s, to allow for some margin.

Table 2 shows the ΔV budget for the Heracles LAE based on mission analysis and updated by means of the results of the Monte Carlo simulations.

Table 2: HERACLES LAE TOTAL MISSION ΔV

		ΔV/ m · s-1	Total plus margin
Transfer phase	**Ascent to CLMO**	1940	2037 (5%)
	Circularization	15.9	16.7 (5%)
	Transfer to NRO injection	654.6	687.3 (5%)
	Correction budget	85.6	85.6
	NRO insertion	34.3	36 (5%)
	Total transfer	2730.4	2862.6
Rendezvous phase	**Segment 1 (S1->S2.1)**	13.9	27.8 (100%)
	Segment 2 (S2.1->S2.2)	5.3	10.6 (100%)
	Segment 3 (S2.2->S3.1)	5	10 (100%)
	Segment 4 (S3.1->S3.2)	1	2 (100%)
	Segment 5 (S3.2->S4)	37.9	45.5 (20%)
	Total rendezvous	63.1	95.9 (100%)
Contingency		25	25
Total		2818.5	2983.5

5 HIL TEST RESULTS

The HIL tests have been performed in the ***platform-art***© facility [7]. The set-up for the HIL tests requires a scaled model of the LOP-G to be fitted with markers. These markers are detected by image processing software and the marker positions in the image plane are fed to the navigation filter. The objectives of the tests are:

- To demonstrate the feasibility of the short-range navigation concept in a low-accuracy set-up
- To validate the image processing algorithm performance in an open-loop test
- To assess the short-range navigation performance with inputs from an image processing function processing real camera images in a low-accuracy set-up
- To assess the performance of the overall GNC system in closed-loop, in a low-accuracy set-up, using real camera images processed by an image processing function as input to the navigation function

The mock-up is a 1:10 scale model of one of the modules of LOP-G, meaning that the linear dimensions of the mock-up are ten times smaller than the true LOP-G. The trajectory to be simulated is also scaled by a **factor of 10**. Any manufacturing errors in the mock-up (including marker placement) will be amplified by a factor of 10 when considering the corresponding errors on LOP-G. This means that the performance of the navigation function with respect to the mock-up will actually be worse than with respect to the LOP-G station. Figure 13 shows a photograph taken of the ***platform-art*** setup at the start of the test campaign.

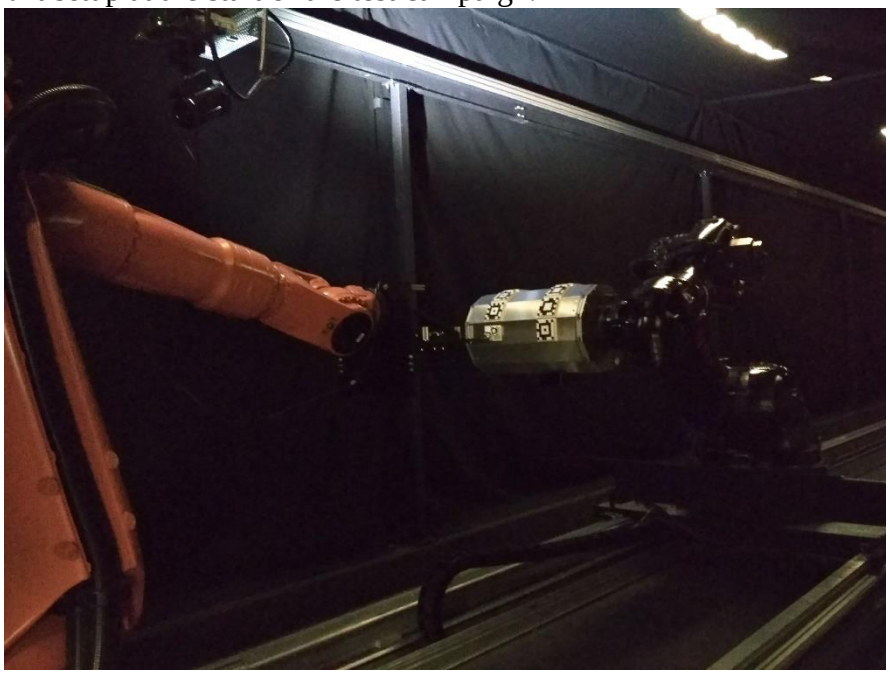

Figure 13: Platform-art test set-up

Figure 14 show the results of the HIL simulations, specifically the target attitude and position estimation errors, including the 3σ bounds. The behaviour is qualitatively very similar to the results obtained during the MIL test campaign. The navigation performance is best between about 500 and 900 seconds. The number of detections start increasing between 400 and 500 seconds, and it is during that interval that the navigation solution improves. After 900 seconds, the solution settles on an offset due to a bias in the marker position. Bias in the model is expected for several reasons:

- LASER calibration equipment was not available, meaning that the positions of markers was established through hand-measurements alone (ruler + calculator)
- The model was not built to exacting standards of precision
- There is reason to suspect a deformation of the model as a whole due to a handling mishap

This means that the bias is entirely due to the hardware used for the test, and that it can be expected that the bias can be greatly reduced if a more meticulous HIL testing campaign is performed.

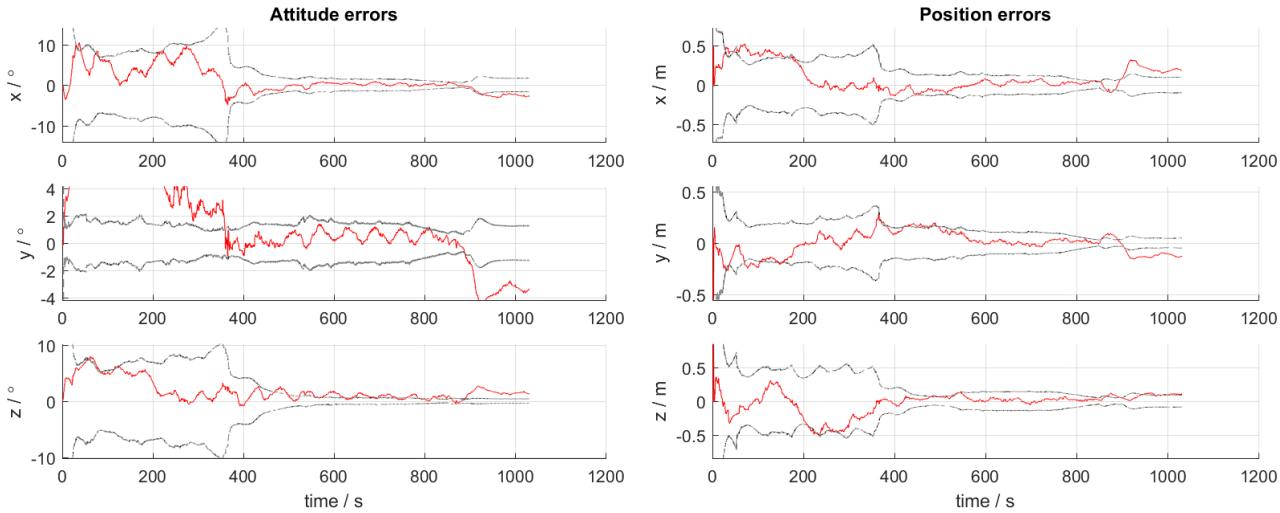

Figure 14: HIL test target attitude and position estimation errors

6 DISCUSSION AND ANALYSIS

Detailed analysis has been performed on the execution of the insertion burn and the propellant consumption for attitude control during the cruise in the transfer orbit and during the short range rendezvous. Figure 15 shows the variation of the propellant consumption during the short range rendezvous under different assumptions. The propellant consumption depends crucially on the assumptions made on the RCS thruster configuration, the trajectory, the attitude motion of the target. The trajectories labelled "guidance integration" represent a direct integration of the feed-forward acceleration provided by the guidance, and can be considered the ideal minimum ΔV required to follow the reference trajectory. Comparison with the other trajectories shows that the principal cause of increase is the geometric losses associated with the RCS thruster configuration. If the chaser needs to follow the attitude motion of the target, then the ΔV increases by about a factor of 4. This is due both to an increase in geometric losses and to additional effort required from the control function.

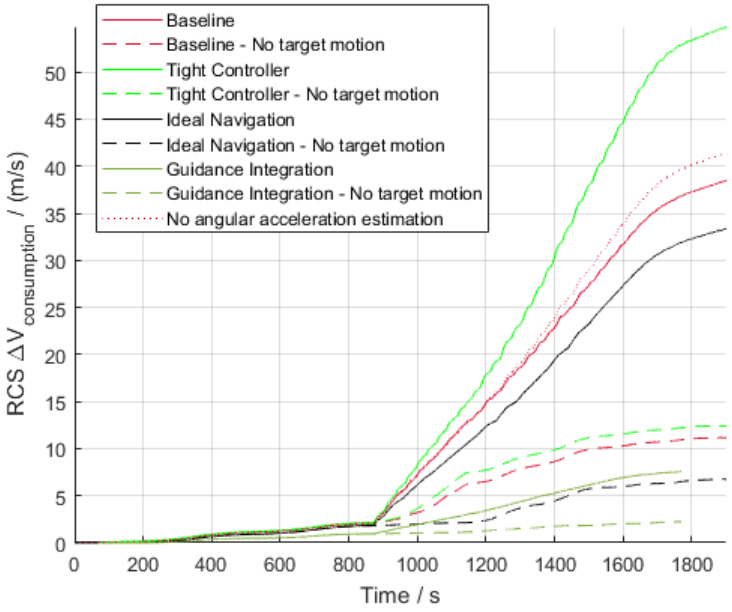

Figure 15: Propellant consumption during short range rendezvous

7 CONCLUSIONS

GNC software has been developed that integrates the GNC for launch and ascent, orbit transfer and rendezvous phases into a single function under the command of an MVM. Monte Carlo test results demonstrate that each of the phases can successfully be performed. The rendezvous is performed with sufficient accuracy to complete the mission. Supporting analyses show that the results are close to the best achievable with the current design of the LAE.

The rendezvous phase GNC is capable of successfully performing the rendezvous with sufficient accuracy at berthing (apart from the attitude rate requirement). The errors in position are smaller than 1 m (3σ), the errors in velocity are smaller than 0.012 m/s (3σ). The angular misalignment is smaller than 5° (3σ), and the angular rate error is smaller than 0.25 °/s (3σ). The original requirement for the angular rate required < 0.04 °/s (3σ), but it was agreed to relax this requirement. The MVM during the rendezvous can successfully command the full rendezvous sequence and it can command a stop at and retreat at any time, meaning that the MVM can successfully execute the rendezvous sequence both forwards and backwards. The MVM can further command the execution of collision avoidance manoeuvres and safe modes during rendezvous.

8 REFERENCES

[1] Peters, T.V., et. al., *GNC For Lunar Ascent, Orbit Transfer and Rendezvous in Near-Rectilinear Halo Orbits*, IAC-19-C1.7.9, proceedings of the 70th International Astronautical Congress, Washington D.C., United States, 2019.

[2] Howell, K.C., 1984, "Three-dimensional, periodic, 'halo' orbits," Celestial mechanics, Vol. 32, Iss. 1, pp.53-71

[3] Howell, K. C. & Pernicka, H. J., *Numerical determination of Lissajous trajectories in the restricted three-body problem*, in: Celestial Mechanics (ISSN 0008-8714), vol. 41, no. 1-4, 1987/88, p. 107-124. Research supported by Computer Sciences Corp.

[4] Lepetit, V., Moreno-Noguer, F. and Fua, P., 2009. "Epnp: An accurate o (n) solution to the pnp problem," International journal of computer vision, 81(2), p.155.

[5] Zamani, M., Trumpf, J., Mahony, R., Nonlinear attitude filtering: a comparison study, arXiv preprint, arXiv:1502.03990.

[6] P. Colmenarejo, M. Graziano, G. Novelli, D. Mora, P. Serra, A. Tomassini, K. Seweryn, G. Prisco, "On Ground Validation of Debris Removal technologies," Proceedings of the 7th European Conference For Aeronautics And Space Sciences (EUCASS), Milan, Italy

[7] P. Colmenarejo, E. di Sotto and J. A. Bejar "Dynamic test facilities as ultimate ground validation step for space robotics and GNC system", 6th ICATT